

UNCLASSIFIED

Defense Technical Information Center
Compilation Part Notice

ADP012174

TITLE: Processing, Dynamic Studies and Properties of Exfoliated
Aerospace Epoxy-Organoclay Nanocomposites

DISTRIBUTION: Approved for public release, distribution unlimited

This paper is part of the following report:

TITLE: Nanophase and Nanocomposite Materials IV held in Boston,
Massachusetts on November 26-29, 2001

To order the complete compilation report, use: ADA401575

The component part is provided here to allow users access to individually authored sections of proceedings, annals, symposia, etc. However, the component should be considered within the context of the overall compilation report and not as a stand-alone technical report.

The following component part numbers comprise the compilation report:

ADP012174 thru ADP012259

UNCLASSIFIED

Processing, Dynamic Studies and Properties of Exfoliated Aerospace Epoxy-Organoclay Nanocomposites

Chenggang Chen¹ and David Curliss²

¹University of Dayton Research Institute, 300 College Park, Dayton, OH 45469-0168, U.S.A.

²Air Force Research Laboratory, Materials and Manufacturing Directorate, WPAFB, OH 45433, U.S.A.

ABSTRACT

Epoxy nanocomposites were prepared from the montmorillonite after organic treatment with a high T_g epoxy resin (Shell Epon 862 and curing agent W). Investigation of the rheological characteristics showed that the addition of clay to the resin did not significantly alter the viscosity or cure kinetics and that the modified resin would still be suitable for liquid composite molding techniques such as resin transfer molding. DSC was performed to study the kinetics of the curing reactions in the modified resin. An *in situ* small-angle x-ray scattering (SAXS) experiment was used to try to understand the structural development during cure. Based on the *in situ* SAXS data, structural changes were monitored in real time during cure and analyzed. Results from wide-angle x-ray diffraction, SAXS, and transmission electron microscopy of the polymer-silicate nanocomposites were used to characterize the morphology of the layered silicate in the epoxy resin matrix. The glassy and rubbery moduli of the polymer-silicate nanocomposites were found to be greater than the unmodified resin due to the high aspect ratio and high stiffness of the layered silicate filler. The solvent absorption in methanol was also slower for the polymer-silicate nanocomposites.

INTRODUCTION

Conventional composite materials are materials with a macroscopic combination of two or more distinct materials, having recognized interface between them [1]. They have been widely used in construction, transportation, electronics and consumer products. Composites with at least one solid phase with a dimension in the range of 1-100 nm can be defined as nanocomposites [2, 3]. Polymer-layered silicate nanocomposites are new hybrid materials of polymers with nanometer-thickness layered silicates. Due to the unique nanometer-size dispersion of the layered silicates with high aspect ratio and high strength in the polymer matrix, these materials generally exhibit improvements in properties even at low loading of layered silicate. These properties can include mechanical performance, ablation performance, thermal stability, barrier performance, and flame retardancy [4-7].

Layered silicates are abundant and important minerals in geological environments at or within roughly 20 km of the Earth surface [8]. There are many types of sheet silicates including clay mineral. The most widely used layered silicate for the nanocomposites is montmorillonite. Natural montmorillonite is constructed of repeating TOT layers composed of two silica tetrahedral sheets fused to an edge-shared octahedral sheet of alumina. The physical dimensions for these silicate sheets are around one hundred to several hundred nanometer in lateral and 1-nm in thickness. However, the individual sheets in the silicates are generally stacked together and hydrophilic, and thus are not compatible with the hydrophobic organic matrix polymer. Therefore, the challenge is to produce a layered silicate system compatible with the matrix

polymer. Fortunately, some silicon atoms in the silica tetrahedral layer and some alumina atoms in the octahedral layer are isomorphically substituted by alumina and magnesium, respectively. This generates negative charges that are counter-balanced by some cations such as Na^+ , K^+ or Ca^{2+} in the gallery. These cations can be easily exchanged with surfactant such as alkyl ammonium cations. The pendent organic group in the surface of the silicate sheets lowers the surface energy of silicate layers and make the layered silicate compatible with polymer matrix. Up to now, extensive research on the polymer layered silicate nanocomposites is being carried out and most of the research is focused on the preparation of the nanocomposite [4-7]. In this research work, the emphasis is placed on aerospace epoxy-silicate nanocomposites. In addition to the preparation and characterization of the nanocomposites, the processing and dynamic study are also performed to understand the exfoliation mechanism. The aerospace epoxy studied here is made from Shell Epon 862 (a low viscosity Bis-phenol F/epichlorohydrin-based liquid epoxy resin) and Epi-Cure curing agent W (diethyltoluenediamine). This epoxy system has high T_g (155 °C) and low-viscosity, which is suitable for resin transfer modeling.

EXPERIMENTAL DETAILS

The resin, cure agent, chemical modifiers and clays used in this research includes Shell Epon 862 (a bis-phenol F epoxy), Epi-Cure curing agent W, *n*-octadecylamine (Aldrich), hydrochloric acid (Aldrich), SNA (Southern Clay Products), and I.30E (Nanacor).

The preparation of organoclay, SC18, was as follows: 21.1 g of *n*-octadecylamine in the 750 mL of ethanol and water mixture solvent (v:v, 1:1) was added with aqueous hydrochloric acid (HCl, 1N, 67.5 mL). The mixture was stirred at ~70 °C. When the solution was clear, 67.5 g of SNA was added to the above mixture solution, and the suspension was continuously stirred for 4 hours at ~70 °C. The resultant mixture was filtered. The solid was washed with a mixture of warm ethanol and water, and dried.

Processing: Desired amount of Epon 862 and the corresponding amount of organoclay was mixed and stirred at ~70 °C. The mixture was degassed in the vacuum oven. Then the corresponding amount of curing agent W was added to the mixture and continued stirring. The resulting mixture was cast between glass plates spaced 0.25 inch apart and cured in a programmable Blue M oven using the following curing cycle: heat the cast in the oven to 121°C over 30 minutes, hold at 121°C for two hours, then heat to 177°C over 30 minutes and hold for another two hours at 177°C, and finally cool the cast in the oven to ambient.

Characterization: Wide-angle x-ray diffraction was performed in the Rigaku x-ray powder diffractometer. The generator power was 40 kV and 150 mA, and the scan mode was continuous with a scan rate of 0.6°/min. The scan 2θ range is from 2° to 10°. Some of small-angle x-ray scattering was performed at National Synchrotron Light Source at the Brookhaven National Laboratory (Beamline X27C with a one-dimensional detector). Some other small-angle x-ray scattering was taken using a flat film Statton camera on a Rigaku RU-200 with $\text{Cu K}\alpha$ as its radiation with a wavelength of 1.5418 Å. The power was 50 kV and 150 mA and the exposure time was around 20 hours. The *in-situ* small-angle x-ray scattering experiment was also performed at National Synchrotron Light Source at the Brookhaven National Laboratory (Beamline X27C with a one-dimensional detector). The mixture of the organoclay with Epoxy and curing agent was mounted on the holder and sample was heated up at 2°C/min. The data was recorded every minute. DSC was performed on a TA Instruments differential scanning calorimeter 2920 modulated DSC at 2°C/min with air sweep gas. The sample for transmission

electron microscopy was microtomed in a Reichert-Jung Ultracut Microtome and mounted on 200 mesh copper grids. Transmission electron microscopy was performed using a Philips CM200 transmission electron microscope. The dynamic mechanical analysis was performed using a RHEOMETRICS ARES dynamic spectrometer using torsion bar geometry at a frequency of 100 rad/sec, a strain of 0.1 percent, and a heating rate of 2°C/min; while the viscosity test was carried out at a RHEOMETRICS ARES dynamic spectrometer using 25-mm diameter parallel plates geometry at a frequency of 10 rad/sec, a strain of 3 percent and a heating rate of 2°C/min.

RESULTS AND DISCUSSION

SC18 is the organoclay prepared from Cloisite Na (CEC: ~ 92 meq/100 g) with *n*-octadecylammonium hydrogen chloride in the laboratory while I.30E is commercially available from Nanocor (CEC ~145 meq/100 g, also treated with *n*-octadecylammonium hydrogen chloride). The wide-angle x-ray diffraction shows that the interplanar spacing SC18 was increased to 18.0 Å from original 10.5 Å of Cloisite Na while the interplanar spacing of I.30E is 22.6 Å. This is consistent with the exchange capacities of their original sodium montmorillonite (92 meq vs 145 meq). These two organoclays are very well compatible with aerospace epoxy resins. A series of aerospace epoxy-organoclay nanocomposites were made with different loadings of SC18 and I.30E. The wide-angle x-ray diffraction of the nanocomposites shows that there is no peak at 2 θ scanning ranging from 2° to 10°, which generally indicates that the interplanar spacing is larger than 44 Å and nanocomposites are considered to be exfoliated structures. In order to confirm the morphology of the nanocomposite, small-angle x-ray diffractions were taken at National Synchrotron Light Source at Brookhaven National Laboratory and Rigaku RU-200, Table I. The interplanar spacing is larger than 100 Å when the organoclay loading is less than eight percent. Even the organoclay loading is as high as 10% for SC18, and 9.0% and 12.0% for I.30E, the interplanar spacing is as large as 90 Å, 88 Å and 68 Å, respectively. With the increment of the organoclay loading, the interplanar spacing began to decrease because of less epoxy resin between the nanosheets at the low loading of the organoclay. The weakness of the peak demonstrates the existence of the disordered structures. In addition, the interplanar spacing of the nanocomposites from the synthetic organoclay (SC18) is larger than those from commercial organoclay (I.30E) although the original interplanar spacing of the synthetic clay (~18 Å) is even smaller than that of commercial organoclay (I.30E, 22.6 Å). This is related to the cation-exchange capacity of the montmorillonite used for making nanocomposites. The higher cation-exchange capacity means that more organic group can be introduced into the gallery and interplanar spacing is also larger (22.6 Å). However, when the organoclay was mixed with epoxy resin, the organoclay with high cation-exchange capacity has more organic groups in the gallery, which perhaps slows the epoxy resin migrating into the gallery [9]. Thus it makes the gallery of the nanocomposite from montmorillonite (I.30E) with high cation-exchange capacity smaller than that with lower cation-exchange capacity (SC18).

Several images of transmission electron microscopy of these nanocomposites are taken. The original aggregates of the silicate sheets are disrupted and each individual sheet with nanometer-thickness was well dispersed in the epoxy resin. Some individual sheets are completely disordered while some still preserve the parallel alignment of layers. This is consistent with the results from small-angle x-ray scattering.

The viscosity study related to the I.30E/Epon862/W and Epon862/W was performed by dynamic mechanical analysis, Figure 1. At room temperature, the viscosity of the

Table I. Small-Angle X-ray Diffraction Data, Storage Moduli and Glass Transition Temperatures (T_g) of the Nanocomposites and Their Pristine Polymer

| Clay | d-Spacing (Å) | | T _g (°C) | G' (dyne/cm ²) | |
|-------------|---------------|--------|---------------------|----------------------------|----------------|
| | NSLS | Rigaku | Tan δ | Glassy (30°C) | Rubber (180°C) |
| NA | | | 154 | 1.14E10 | 1.03E8 |
| 1.0% SC18 | 249 | | | | |
| 3.0% SC18 | 135 | 135 | 145 | 1.23E10 | 1.39E8 |
| 6.0% SC18 | 129 | | 154 | 1.30E10 | 2.14E8 |
| 8.0% SC18 | 114 | | | | |
| 10.0% SC18 | 90 | 89/44 | 144 | 1.56E10 | 2.82E8 |
| 1.0% I.30E | 172 | | 153 | 1.20E10 | 1.24E8 |
| 3.0% I.30E | 126 | 125 | | | |
| 6.0% I.30E | 100/49 | 100/48 | | | |
| 9.0% I.30E | | 88/44 | 144 | 1.61E10 | 2.31E8 |
| 12.0% I.30E | | 68 | | | |

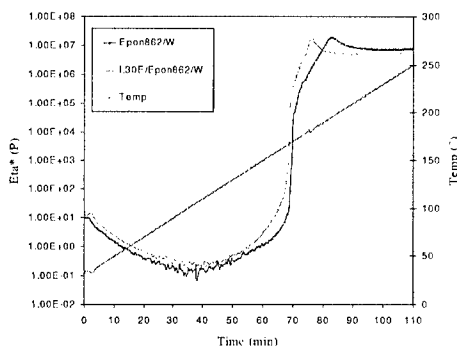


Figure 1. Viscosity of Epon862/W and 6% I.30E/Epon862/W at heating rate (2° C/min).

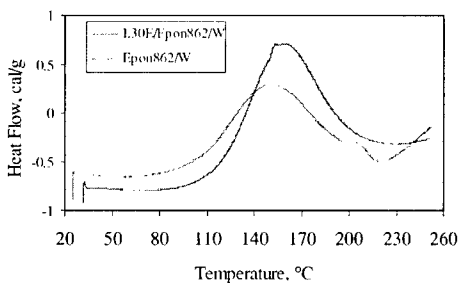


Figure 2. DSC of Epon862/W and 6% I.30E/Epon862/W at heating rate (2° C/min).

I.30E/Epon862/W is a little larger than that of Epon862/W as expected. However the increase is limited and the processable window is still wide for resin transfer modeling. As the temperature increases, the cross-linking polymerization takes place. After the polymer is formed, with the temperature continually increased the solid polymer will begin to soften into rubber state and the viscosity will be decreased to some extent. The shape of the viscosity vs. time and temperature are similar. The gelling takes place more quickly for the epoxy resin with organoclay. The time and temperature of the turning point of softening for I.30E/Epon862/W are also similar to that of Epon862/W, but are clearly shorter (7 minutes shorter) and lower (180 vs. 196 °C). This demonstrates that the organoclay has some catalytic effect on the polymerization of Epon862/W.

The DSC experiment of I.30E/Epon862/curing agent W and Epon862/curing agent W was performed. The DSC was shown in Figure 2. With the addition of the organoclay (I.30E) to the original Epon862/W resin, the nanocomposite system produces more exothermal heat

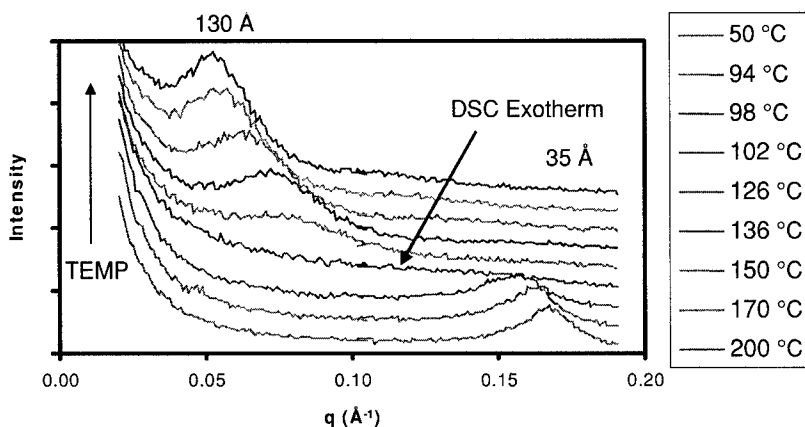


Figure 3. The *in-situ* small-angle x-ray scattering of 6% I.30E/Epon862/W at heating rate ($2^{\circ}\text{C}/\text{min}$).

(49.2 vs 45.7 cal/g) at lower curing onset temperature (102.5 vs 122.5°C). This demonstrates that the organoclay has some catalytic effect on the cross-linking polymerization of Epon862 with curing agent W. This catalytic effect of the organoclay is consistent with the report for the rubber state epoxy system [10].

During processing, the morphology of the system changes. Since the organoclay has layered structure, the gallery interplanar spacing will change. The *in-situ* small-angle x-ray scattering at National Synchrotron Light Source at the Brookhaven National Laboratory provides powerful tools to monitor the structural evolution of the nanocomposite. The Epon 862 and organoclay was mixed in advance. When the corresponding curing agent W was added, the mixture was immediately mounted on the holder. The sample was heated at $2^{\circ}\text{C}/\text{minute}$. In order to be clear, some key data was chosen, Figure 3. When the Epon862 mixed with I.30E, the organoclay after organic treatment was compatible with the epoxy resin. Some epoxy resin will enter into the gallery of the clay. The interplanar was increased to 35 \AA from original 22 \AA . When the mixture was heated up at $2^{\circ}\text{C}/\text{min}$, for the I.30E/Epon862/W, the peak gradually shifts and becomes a little weaker, but not significantly. Amazingly, at $\sim 102^{\circ}\text{C}$, suddenly the ordered structure was collapsed and the exfoliation takes place. Later, a new clear peak appears and the intensity and interplanar spacing in increased gradually. The temperature for the collapse of the ordered structure is the same as the curing onset temperature from DSC. This is perhaps because the exothermal heat from curing at $\sim 102^{\circ}\text{C}$ provides enough energy to make the nanoclay sheets expand quickly and exfoliation takes place. The results of the kinetics studies from *in-situ* small-angle x-ray scattering, DSC and rheological are well related.

The dynamic mechanical analysis, Table 1, shows that the storage modulus of the nanocomposites is higher than that of the pristine epoxy resin. Moduli increase with increased organoclay loading. Generally, the nanocomposites shows more significant improvement of storage modulus in the rubber state than that in the glassy states. The dynamic storage modulus can be increased up to more than 40% in the glassy state and 125% in the rubber state. This is

due to the high aspect ratio and high stiffness of the organoclay filler. The extra reinforcement from further nanosheet alignment in the rubber state perhaps is the reason for larger increase in the rubber state [11].

The effect of the addition of organoclay on the solvent uptake properties of Epon 862/W was examined. Three Epon 862/W panels were made with 0%, 3% and 6% I.30E. The degree of solvent uptake was evident due to the increased mass of the coupons over time. After 60 days, the percent mass gain is 14%, 10%, and 8% for 0%, 3%, and 6% I.30E/Epon862/W; respectively. The reduced transport rates observed for the polymer-silicate nanocomposites were attributed to the hindered diffusion pathways caused by the dispersion of the individual nanosheets of the layered silicate in the nanocomposites.

CONCLUSIONS

Exfoliated aerospace epoxy organoclay nanocomposites are successfully made. The characterization from wide-angle x-ray diffraction, small-angle x-ray diffraction and transmission electron microscopy confirms the exfoliated nanostructure. Rheological, DSC and *in situ* small-angle x-ray scattering study shows that the organoclay has some catalytic effect for polymerization and that the exothermal heat at onset curing temperature is a key factor for nanosheets exfoliation. The morphology of the nanocomposites is also closely related to the CEC of the montmorillonite. The clay with lower CEC is more favorable for the polymer penetration. The dynamic storage of the nanocomposites was increased and the solvent absorption in methanol was slower for the nanocomposites.

ACKNOWLEDGEMENTS

This material is based in part upon the work supported by Air Force Research Laboratory, Materials & Manufacturing Directorate (F33615-00-D-5006), and the Air Force Office of Scientific Research. Authors would also like to thank Dr. Richard Vaia and Dr. Dave Anderson for their help.

REFERENCES

1. T.J. Reinhart, *Engineered Materials Handbook, Vol. 1, Composites Materials* (ASM International, 1987).
2. B.M. Novak, *Adv. Mater.* **5**, 422 (1993).
3. R.F. Ziolo, E.P. Giannelis, B.A. Weinstein, M.P. O'Horo, B.N. Granguly, V. Mehrot, M.W. Russell, D.R. Huffman, *Science* **257**, 219 (1992).
4. W.D. Nesse, *Introduction to Mineralogy*, (Oxford University Press, Oxford, 2000) p. 235.
5. E.P. Giannelis, *Adv. Mater.* **8** (1), 29 (1996).
6. P.C. LeBaron, Z. Wang, T. J. Pinnavaia, *Applied Clay Science* **15**, 11 (1999).
7. J.W. Gilman, *Applied Clay Science* **15**, 31 (1999).
8. M. Alexandre, P. Dubois, *Materials Science and Engineering* **28**, 1 (2000).
9. X. Kornmann, H. Lindberg, L.A. Berglund, *Polymer* **42**, 1303 (2001).
10. T. Lan, P.D. Kavirayna, T.J. Pinnavaia, *J. Phys. Chem. Solids* **57**, 1005 (1996).
11. P.B. Messersmith, E.P. Giannelis, *Mater. Chem.* **6**, 1719 (2001).